Background Removal in Dental Panoramic X-ray Images by the A-Trous Multiresolution Transform

Peter Michael Goebel, †* Ahmed Nabil Belbachir † Michael Truppe ‡

Abstract — **Dental Panoramic X-ray images are images having complex content, because several layers of tissue, bone, fat, etc. are superimposed. Non-uniform illumination, stemming from the X-ray source, gives extra modulation to the image, which causes spatially varying X-ray photon density. The interaction of the X-ray photons with the density of matter causes spatially coherent varying noise contribution. Many algorithms exist to compensate background effects, by pixel based or global methods. However, if the image is contaminated by a non-negligible amount of noise, that is usually non-Gaussian, the methods cannot approximate the background efficiently. In this paper, a dedicated approach for the removal of a multiplying background is presented using polynomial scaling and the A-Trous multiresolution transform. The new method uses a background image and a diagnostic image together to estimate the density of the diagnostic content. It assumes a locally Gaussian statistic scaled by a hidden factor, where the hidden factor represents the variance of the non-Gaussian process of image generation. Because, the method also removes noise from the compound signal, a comparison to a standard denoising method is given. This approach has been tested on 50 images from a database of panoramic X-ray images where the results are cross validated by medical experts.**

1 INTRODUCTION

Non-uniform illumination of any kind generates non-uniform background in an image. The term background comes from the usual classification of the image data into regions of interest and unwanted regions, referred foreground and background, respectively [10]. In [12] the background is defined to be the *bright* surrounding area of the X-ray film viewing box, where the X-ray film size is smaller than that viewing box. The proposed, new approach is different in that it removes also unwanted modulation from the image of interest.

1.1 Background Removal Methods

There exist Non-parametric [7], Pixel Based (like Kalman filtration [8] or Adaptive Thresholding [9]) and Global Methods, which generate the rules for the adaption of the background estimate from some measurable image attributes.

A polynomial fit to a number of points associated with the background is appropriate when the non-uniformity is additive, and the resulting polynomial surface is subtracted from the whole image. For multiplicative non-uniformity, a correction image is generated, corresponding to the polynomial surface. The correction image has factors that represent the ratio of brightness between the non-uniform image and the uniform one and is applied to scale the original image values appropriately.

1.2 Basics of Panoramic Radiography

Dental Panoramic Radiography (DPR) is a technique where the entire dentition is projected onto a sensing device. The physics of such a radiographic process can be subdivided into X-ray source, interaction of the beam with matters and imaging of the surviving photons. Source and detector are in opposition, rotated around the patients head. The focal area of the X-ray beam describes a planar curve, which is standardized for the human teeth and jaws. The photon attenuation of each type of matter depends on its elementary and chemical composition as well as the beam. This effect is quantified by the linear mass attenuation coefficient μ, which gives the fraction of photons that are absorbed by unit thickness of matter [5], which varies by photoelectric absorption, coherent scatter, Compton scatter and the energy spectrum of the beam [1, 3].

1.3 Image Degradation

In [3] the authors of this paper introduced a noise estimation model for DPR. It models the probabilities for scattering events and generates a scatter prior table, which is used together with a background and a diagnostic image to estimate the amount of scatter-glare. The spatially varying contribution of noise is modeled by local Gaussian random variables $N(0,1)$, modulated by hidden factors ξ, representing the variance of every pixel in the image. Only photons absorbed by matter generate good image contrast. During a DPR scan of the entire dentition, the photon rate has to be increased, when the X-ray beam crosses bones from the spine

*fh-campus wien, Technical Project- and Process management, Ettenreichgasse 45a, 1100 Vienna, Austria.

†Vienna University of Technology, Pattern Recognition and Image Procesing Group, Vienna, Austria, e-mail: [goe,nabil]@prip.tuwien.ac.at, tel.: +43 1 58801-18362, fax: +43 1 58801-18392.

‡Karl Landsteiner Institute for Biotelematics, Danube University Krems, A-3500 Krems, Austria, e-mail: mtruppe@biotelematics.at

region. Thus a non-uniform illumination of the radio graph is caused, leading to extra modulation of the image.

In this paper, a dedicated approach for the removal of a multiplying background is presented using polynomial scaling and the A-Trous multiresolution transform.

2 THE METHOD EXPLAINED

As the geometry of the DPR system is fixed, a scan, taken without a patient gives an estimate for the background.

2.1 The Image Model

The X-ray generator in Figure 1 produces photons with intensity I_0, which travel through collimator and filter to the patient. The intensity I_1 can be measured incidently to the patient and is the patient's photon input energy. Suppose this energy interacts with the different layers i of K matters, of thickness d_i and attenuation μ_i inside the patient, then one can measure I_2 at the sensor.

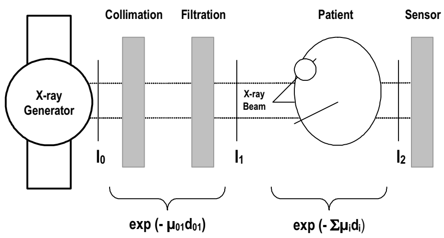

Figure 1: Outline of the X-ray Physics.

Care has to be taken, removing the multiplying background, to not overcompensate the spine region (see section 1.3). Formulating the physical situation of Figure 1 into mathematical terms of linear attenuation coefficients, gives

$$I_2 = \underbrace{I_0 \cdot \underbrace{\exp(-\mu_{01}\, d_{01})}_{background\, scatter}}_{I_1} \cdot \underbrace{\exp(-\sum_{i=1}^{K}(\mu_i\, d_i)}_{diagnostic\; scatter} \quad (1)$$

In (1) the intensity I_2 at the sensor is decomposed into the background part I_1 (Figure 3) and is attenuated by the diagnostic part, which is that of interest (Figure 4 top). The Inversion of (1) leads to

$$\frac{I_2}{I_1} = \exp\left(-\sum_{i=1}^{K}(\mu_i\, d_i)\right) \quad (2)$$

Where in (2) the $\sum ...$ represents the total diagnostic cross section of the image and the fraction $\frac{I_2}{I_1}$ is in effect the optical transmittance of the patient. Concerning an evenness criteria, the non-uniformity is compensated by fitting two polynomials p_1 and p_2 of order 2 and 17, respectively, to the vertical profile of the transmittance $\frac{I_2}{I_1}$. Correction factors $F_k = \frac{p_2}{p_1}$ are then applied to gain image $I_1' = I_1 F_k$ and the compensated transmittance image $\frac{I_2}{I_1'}$ (Figure 4 bottom). Since I_1' and I_2 are individual samples, assuming statistical independence, the noise variance for $\frac{I_2}{I_1'}$ is given from [6]

$$\sigma^2 \cong \frac{\sigma_2^2}{m_1^2} + \left(\frac{m_2}{m_1^2}\right)^2 \sigma_1^2 \quad \overset{Median(I_1')}{\underset{\sigma_1=0}{\rightarrow}} \quad \sigma^2 \cong \frac{\sigma_2^2}{m_1^2} \quad (3)$$

In (3) the noise contribution σ^2 of (2) is determined, where σ_j^2 and m_j $(j = 1, 2)$ is the local variance and the local mean of I_1' and I_2, respectively. Filtering I_1' by a median 9x9 filter sets $\sigma_1^2 = 0$, thus the noise variance from (2) is only scaled by the local mean m_1 and one can define the additive noise model

$$\left(\frac{I_2}{I_1'}\right) = T + \xi_{xy}\left(\sigma^2\right)\, N(0,1) \quad (4)$$

Where T is the noise free transmittance image, xy are pixel coordinates. The spatially varying σ^2 from (3) is modeled by a locally Gaussian random field with scale factors $\xi(xy)$ and locally Gaussian noise $N(0, 1)$. Thus, subtracting that field of randoms will reconstruct properly the image T.

2.2 Shrinking Method for the Wavelet Coefficients by Preservation of Energy

Subtracting the noise contribution from (4) directly from the transmittance T usually increases the noise contribution in the difference image, because noise cannot be subtracted from noise in the spatial domain. Therefore, it is more convenient to perform this subtraction in another domain. The A-Trous multi resolution transform [4] is used to form an undecimated, over complete representation, by decomposing the image into different contributions in several frequency bands and at different scales.

Following (4), the idea is to subtract from the energies of the mixture the energies of the noise.

Stressing Plancherel's Theorem [11] for non-orthogonal discrete wavelets and $M < \infty$ finite scales, using the $L^2(\Re)$ norm, yields to

$$\|s\|^2 = \underbrace{C_E \sum_{i=0}^{M-1} \frac{1}{2^i} \|w_i\|^2}_{coefficients\; energy} + \underbrace{\frac{1}{2^M} \|r_M\|^2}_{resid.\; energy} \quad (5)$$

where w_i are the wavelet coefficients of the i^{th} scale, r_M is the residual scale and $\int \|s\|^2$ would be the signal energy in the spatial domain. The constant C_E in (5) is chosen for conservation of energy and is determined for M=1 and an input impulse function $s = \delta$, getting $\|s\| = 1$ (see [11] for more details).

Calculating the energies, using (5), gaining E_N from the noise estimate of (4), the energy of the output image $E_{\widehat{Z}}$, and making up the balance by the norm of the energies, leads to the energy of the diagnostic mixture (E_D) with the noise removed

$$\|E_{D_{x,y}}\| = \left\|E_{\widehat{Z}_{x,y}}\right\| - \|E_{N_{x,y}}\| \tag{6}$$

From the reconstructed energy E_D, shrinkage weighting factors, for $\left\|E_{\widehat{Z}_{x,y}}\right\| > 0$ are introduced to convey the result to the coefficients:

$$f_{D_{x,y}} = \frac{\|E_{D_{x,y}}\|}{\left\|E_{\widehat{Z}_{x,y}}\right\|} \tag{7}$$

The corrected coefficients are calculated now, by application of the shrinkage weights

$$\breve{w}_{i_{x,y}} = w_{i_{x,y}} \cdot f_{D_{x,y}} \tag{8}$$

Then, the usually reconstruction of the A-Trous multiresolution transform yields to the reconstructed image I_R

$$I_R = \sum_{i=0}^{M-1} \breve{w}_i + r_M \tag{9}$$

In the following a simulation illustrates the method.

2.3 A Mixing Simulation Example

Consider an image with a gently inclining gray level ramp, and another image, having a gray level checkerboard. From the checkerboard two images are produced, corrupted by two independent instances of Poisson noise.

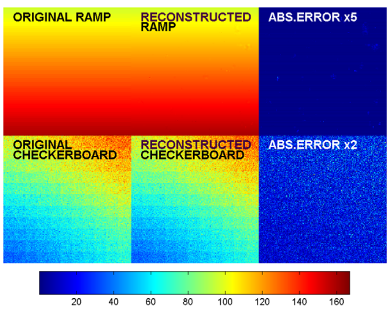

Figure 2: Simulation of the method.

Figure 2 shows the experiment, the images at the left are added to form the mixture. In the middle, as cross validation, the proposed method reconstructs the gray ramp image (top) and the checkerboard image (bottom) from the one mixture. At right the images of the reconstruction errors show that the method properly distinguishes the two images, including the noise contribution of the gray checkerboard image.

3 ANALYSIS AND RESULTS

In this section the results of the background removal of a DPR image and a 5-layer test phantom [Quart (Ltd.), Germany, 2004].

3.1 Polynomial Background Correction

Figure 3 shows a background image, where one can see the non-uniformity of the X-ray illumination.

Figure 3: Background image I_1.

Top of Figure 4 shows a diagnostic image. Firstly the background image is registered with the diagnostic image, then the polynomial correction (see section 2.1) is applied, the result is shown in Figure 4 bottom. One can see the more evenly distributed contrast in the bottom image. There are no artifacts from the background polynomial correction.

3.2 Removal of the Noise Contribution

The algorithm, explained in section 2 is applied to the Quart phantom, which is put in place of the patient's jaws. The phantom has a well defined structure and one is able to determine several characteristic properties of the scanner system itself (e.g. modulation transfer function (MTF), etc.).

Four stripes are shown in Figure 5: a) the result of a spatial background subtraction; b) the original image; c) the result of the application of a standard stationary wavelet (SWT) denoising by a Daubechies wavelet db3 and soft thresholding at 3 scales [2]; and d) the result of the new method. At the top of every stripe, a zoomed view from the $2.5\frac{lines}{mm}$ sine gratings of the phantom is shown, and at the right hand side, an intensity plot of the sine gratings are shown. The modulation transfer function (MTF) for a frequency of $2.5\frac{lines}{mm}$ gives: 53% for the unprocessed image b), 21% for SWT method

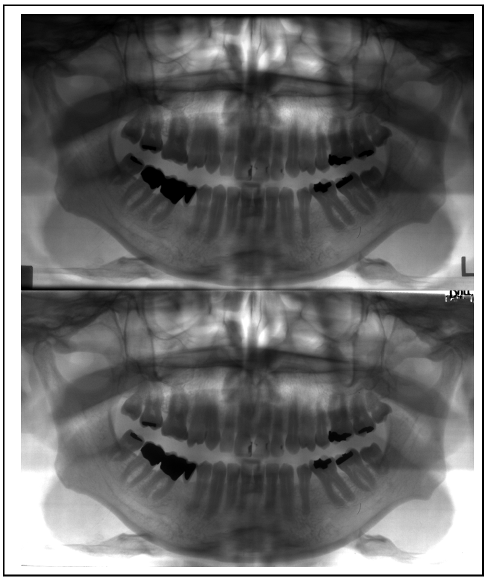

Figure 4: DPR Images top: I_2 unprocessed; bottom: polynomial compensated transmittance $\frac{I_2}{I_1'}$.

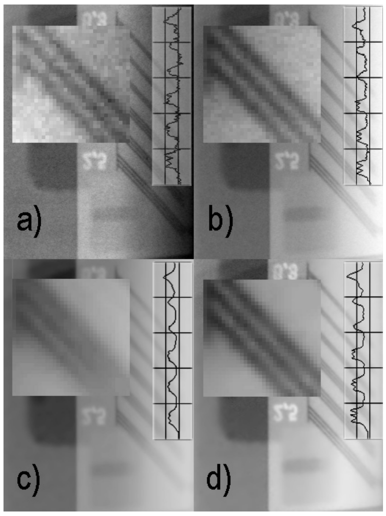

Figure 5: A comparison by MTF patterns of the results: a) spatially method, b) original, c) SWT denoised, d) new method.

c), and 44% for the proposed method d), which preserves image contrast and small details better than the SWT method.

4 CONCLUSIONS

In this paper, a new method for the removal of a multiplying background in dental panoramic X-ray by polynomial scaling and shrinking the wavelet coefficients under the constraint of preservation of energy is given. It is shown, that an adaptive polynomial correction gives a good result for compensation of the non-uniform illumination.

A new method is proposed to remove the contributions of noise in the wavelet domain. The method is compared to a spatial background correction method and to a standard denoising method, in fact the results show improved quality in either case. Considering terms of MTF, fine and weak details are preserved by better support for high frequency information, applying the method.

References

[1] Aird EGA. Basic Physics for Medical Imaging. *Heinemann, Oxford, 1988*

[2] D.L. Donoho. Denoising by Soft-thresholding. *IEEE Trans. on Information Theory, Vol.41, pp.613-627, 1995*

[3] P.M. Goebel, A. N. Belbachir, M. Truppe. Noise estimation in panoramic X-ray images: An application analysis approach. *Workshop on Statist. Signal Processing, SSP05, Bordeaux, 17-20 July, 2005*

[4] M. Holschneider, R. Kronland-Martinet, J. Morlet, and Ph. Tchamitchian. A real-time algorithm for signal analysis with help of the wavelet transform. *Wavelets, Time-Frequency Methods and Phase Space, Berlin: Springer, IPTI, 1989, pp. 286-297.*

[5] J. H. Hubbell, S. M. Seltzer Tables of X-Ray Mass Attenuation Coefficients and Mass Energy-Absorption Coefficients (version 1.4). *NISTIR 5632, NIST, Gaithersburg, MD (1995).*

[6] A. T. Langewisch, F. F. Choobineh. Mean and Variance Bounds and Propagation for Ill-Specified Random Variables. *IEEE Trans. on Systems, Man and Cybernetics, Vol. 34, No.4, July 2004.*

[7] W. Long and Yee-Hong Yang. Stationary background generation: an alternative to the difference of two images. *Pattern Recogn., 23(12):1351–1359, 1990.*

[8] C. Ridder, O. Munkelt, H. Kirchner. Adaptive Background Estimation and Foreground Detection using Kalman-Filtering. *Proc. Int. Conf. on recent Adv. in Mechatr. ICRAM'95, 193-199, 1995.*

[9] A. E. Savakis Adaptive document image thresholding using foreground and background clustering. *1998 Int. Conf. on Image Proc. (ICIP '98) October 04-07, 1998.*

[10] A. J. Shelley, N. L. Seed. Approaches to Static Background Identification and Removal. *Journal of the Institution of Electrical Engineers, IEE, 1993.*

[11] M. J. Shensha. Discrete Inverses for Nonorthogonal Wavelet Transforms. *IEEE Transactions on Signal Processing, vol. 44, no. 4, pp. 798-807, April 1996.*

[12] J. Zhang and H. K. Huang. Automatic Background Recognition and Removal (ABRR) in Computed Radiography Images. *IEEE Trans. on Medical Imaging, Vol. 16., No. 6., December 1997.*